TeV halo candidate surrounding PSR J0359+5414 detected with the HAWC observatory

Sara Coutiño de León
University of Wisconsin-Madison

on behalf of HAWC collaboration

7th Heidelberg International Symposium on High-Energy Gamma-Ray Astronomy (γ-2022)
July 5th, 2022

Introduction

TeV halos are extended gamma-ray emission found around middle-aged pulsars.

Name	RA	Dec	Type Tags	Distance	Catalog
HAWC J0543+233	05 43 07.2	+23 24 00	Gal,TeVHalo	z=0.0	Newly Announced
LHAASO J0621+3...	06 21 52.8	+37 55 12	Gal,PWN,T...	z=0.0	Default Catalog
Geminga	06 32 28	+17 22 00	Gal,SNR,P...	0.25 kpc	Default Catalog
HAWC J0635+070	06 34 50.4	+07 00 00	UNID,TeVH...	z=0.0	Newly Announced
2HWC J0700+143	07 00 28.8	+14 19 12	Gal,TeVHalo	z=0.0	Default Catalog
Vela X	08 35 00	-45 36 00	Gal,SNR,P...	0.29 kpc	Default Catalog
HESS J1825-137	18 25 49	-13 46 35	Gal,SNR,P...	3.9 kpc	Default Catalog

TeV halo list from the TeVCat: http://tevcat2.uchicago.edu/

TeV halo detections are important to:

- constrain the halo production mechanism,
- and to determine if this a generic feature of middle-age pulsars.

Introduction

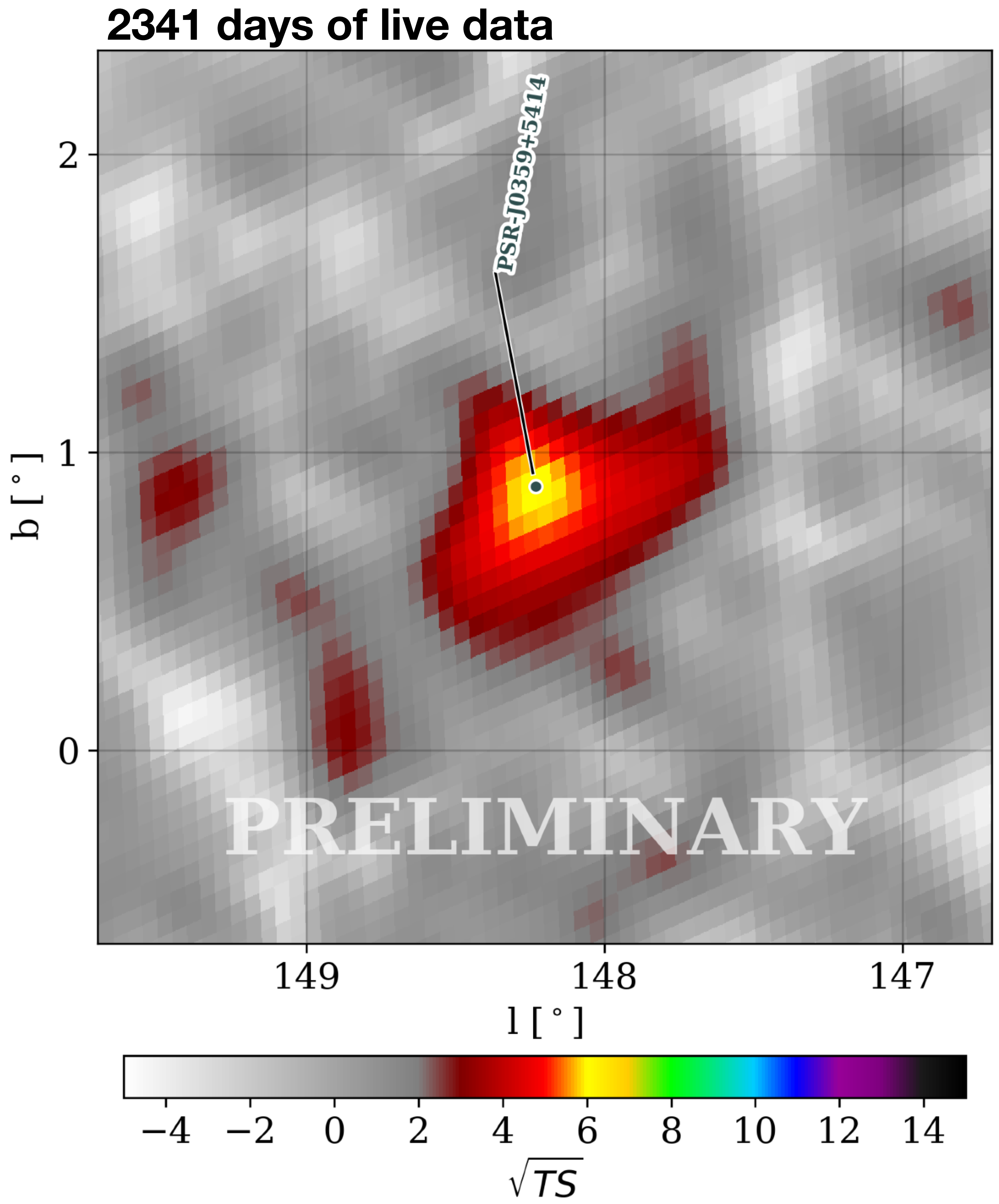

- PSR J0359+5414 is a radio-quiet pulsar
- Spin-down power $\dot{E} = 1.3 \times 10^{36}$ erg/s.
- Distance $d = 3.45$ kpc.
- Age = 75 kyr.
- The PWN associated to this source has been observed in X-rays with a ~ 30 arcsec size (Zyuzin et al. 2018).
- Detected by Fermi-LAT
- At VHE has not been detected before by any IACT or EAS experiment.
- HAWC detects an excess above 6σ in the 15-78 TeV energy range.

Analysis method

We performed spectral and spatial fits using a maximum likelihood technique

Spectral models:

1. $$\frac{dN}{dE} = N_0 \left(\frac{E}{E_0}\right)^{-\alpha}$$ —> power law (PL)

2. $$\frac{dN}{dE} = N_0 \left(\frac{E}{E_0}\right)^{-\alpha-\beta \ln(E/E_0)}$$ —> log-parabola (LOGP)

3. $$\frac{dN}{dE} = N_0 \left(\frac{E}{E_0}\right)^{-\alpha} \times \exp\left(\frac{-E}{E_c}\right)$$ —> power law with exponential energy cutoff (PL+CO)

Spatial models:

1. Point-like
2. Extended —> Symmetric Gaussian

N_0, α, β, E_c left free in the fit
Pivot energy E_0 fixed at 30 TeV to minimize correlations with the other parameters

Results

Model	TS	ΔBIC	Extension	N_0	α	β	E_c
			[$\circ$]	[$\times 10^{-16}$TeV^{-1}cm^{-2}s^{-1}]			[TeV]
PL, point-like	37.86	12	0.0	$1.34^{+0.34}_{-0.27}$	2.60 ± 0.16	-	-
LOGP, point-like	39.18	1	0.0	$1.6^{+0.5}_{-0.4}$	2.80 ± 0.23	0.14 ± 0.12	-
PL+CO, point-like	37.98	0	0.0	4^{+50}_{-4}	2.5 ± 1.2	-	10^8
PL, extended	40.27	12	0.2 ± 0.1	$2.0^{+0.8}_{-0.6}$	2.52 ± 0.16	-	-
LOGP, extended	41.72	1.2	0.2 ± 0.1	$2.6^{+1.5}_{-1.0}$	2.71 ± 0.22	0.14 ± 0.13	-
PL+CO, extended	40.48	0	0.23 ± 0.10	14^{+5}_{-4}	2.40 ± 0.19	-	270^{+240}_{-130}

NOTE—ΔBIC is obtained from the comparison with the model with the highest BIC, which from both spatial models is the PL+CO spectral model.

Results

Model	TS	ΔBIC	Extension [$\circ$]	N_0 [$\times 10^{-16}$TeV^{-1}cm^{-2}s^{-1}]	α	β	E_c [TeV]
PL, point-like	37.86	12	0.0	$1.34^{+0.34}_{-0.27}$	2.60 ± 0.16	-	-
LOGP, point-like	39.18	1	0.0	$1.6^{+0.5}_{-0.4}$	2.80 ± 0.23	0.14 ± 0.12	-
PL+CO, point-like	37.98	0	0.0	4^{+50}_{-4}	2.5 ± 1.2	-	10^8
PL, extended	40.27	12	0.2 ± 0.1	$2.0^{+0.8}_{-0.6}$	2.52 ± 0.16	-	-
LOGP, extended	41.72	1.2	0.2 ± 0.1	$2.6^{+1.5}_{-1.0}$	2.71 ± 0.22	0.14 ± 0.13	-
PL+CO, extended	40.48	0	0.23 ± 0.10	14^{+5}_{-4}	2.40 ± 0.19	-	270^{+240}_{-130}

NOTE—ΔBIC is obtained from the comparison with the model with the highest BIC, which from both spatial models is the PL+CO spectral model.

Results

PL & point-like model

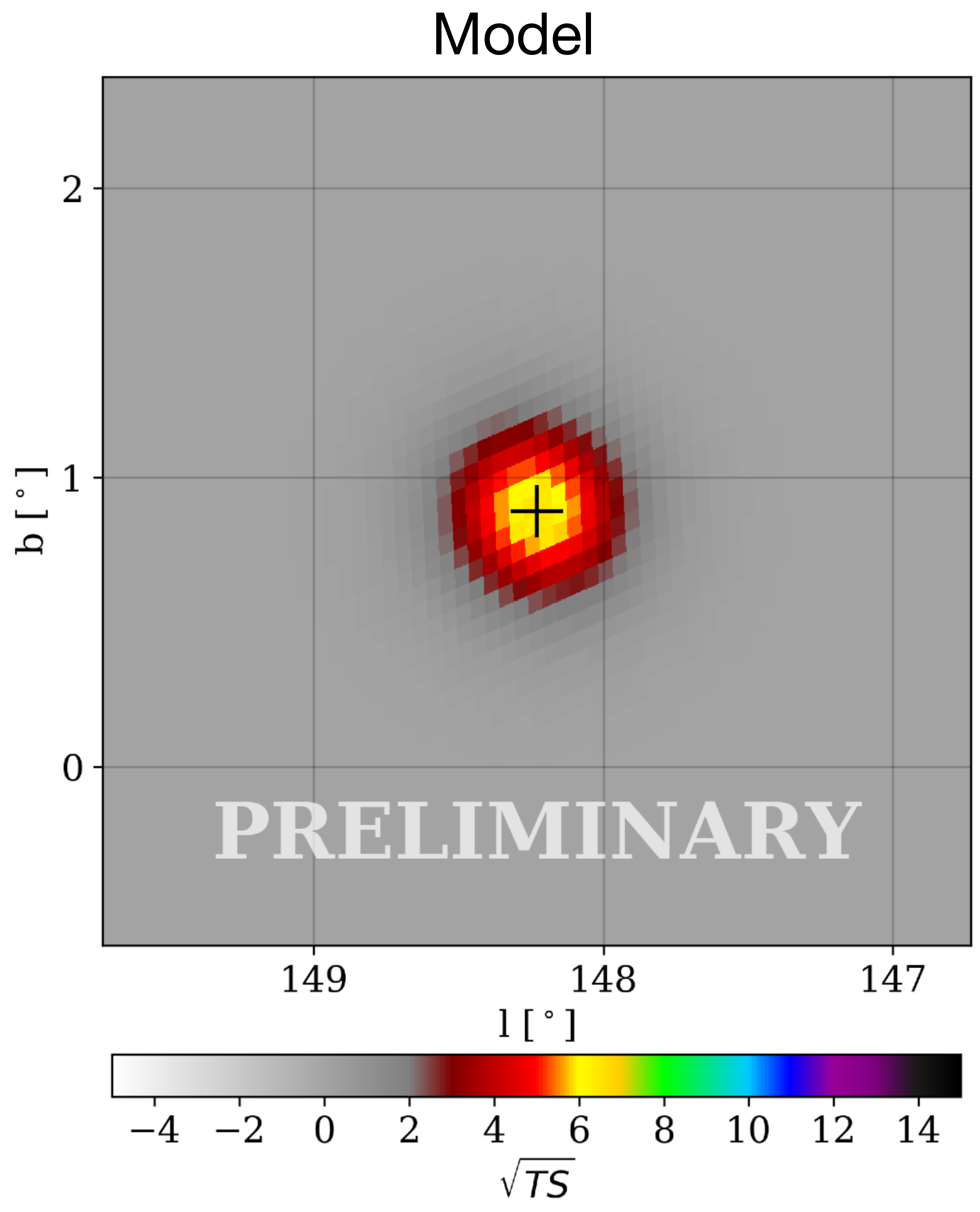

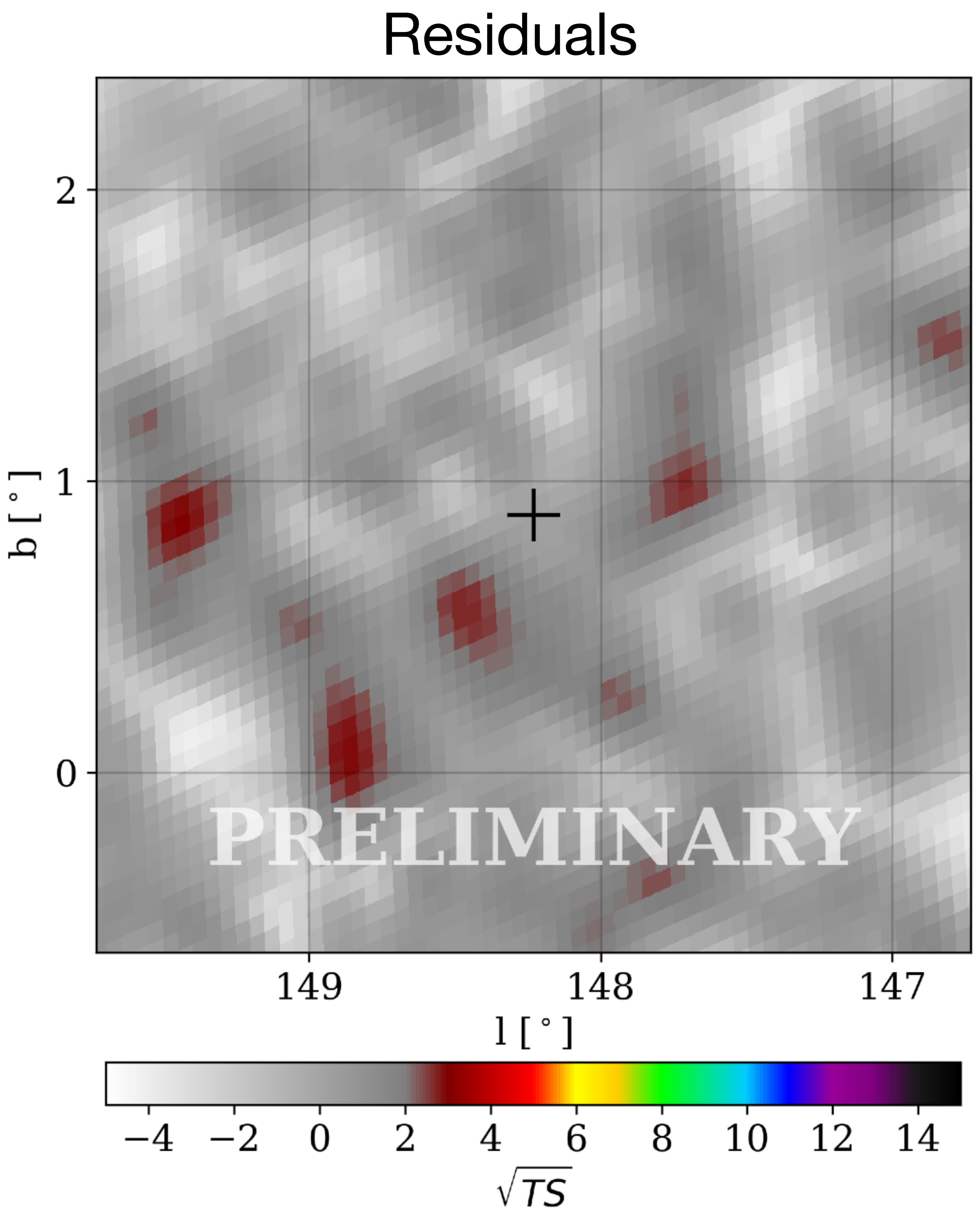

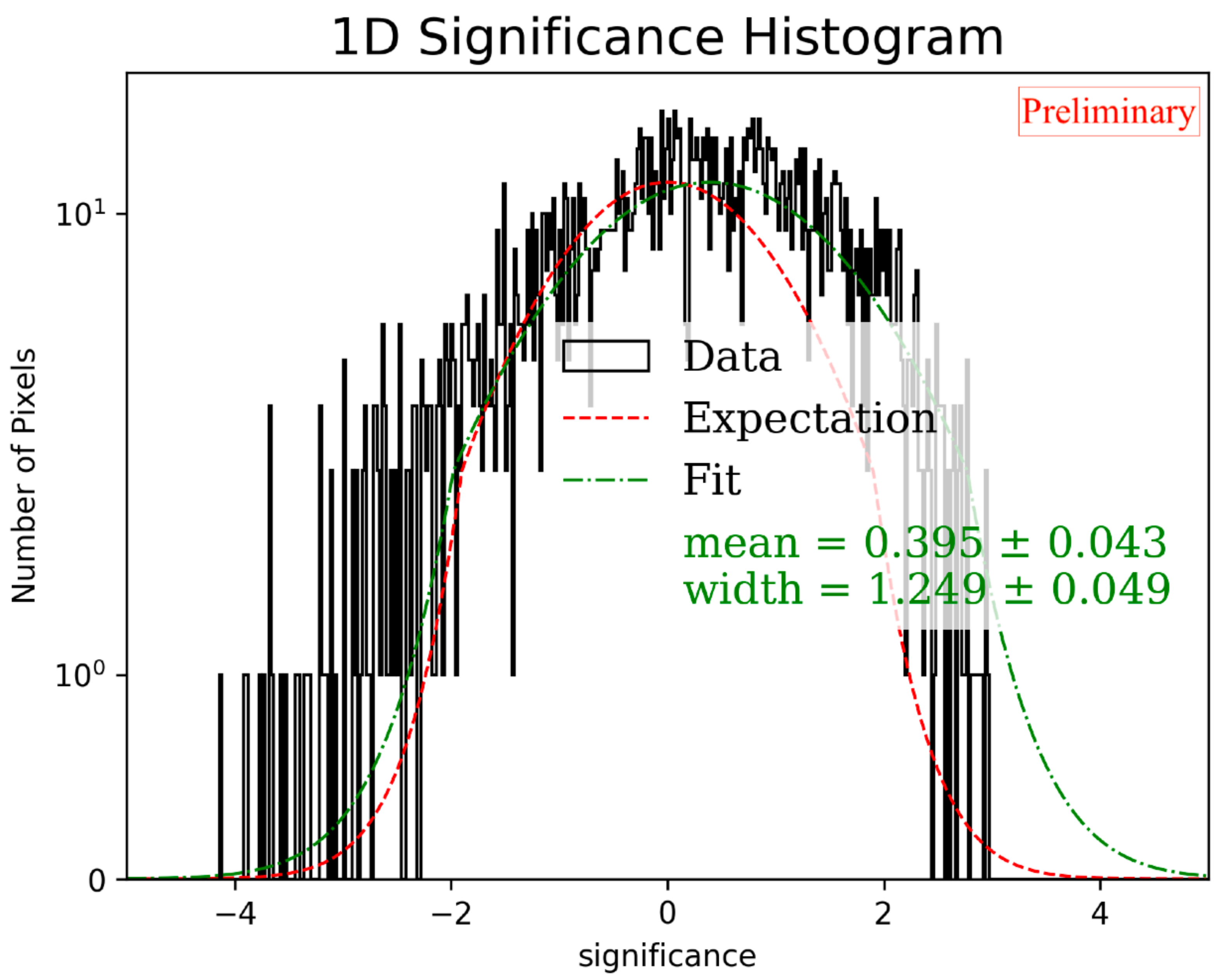

Results

PL & extended model

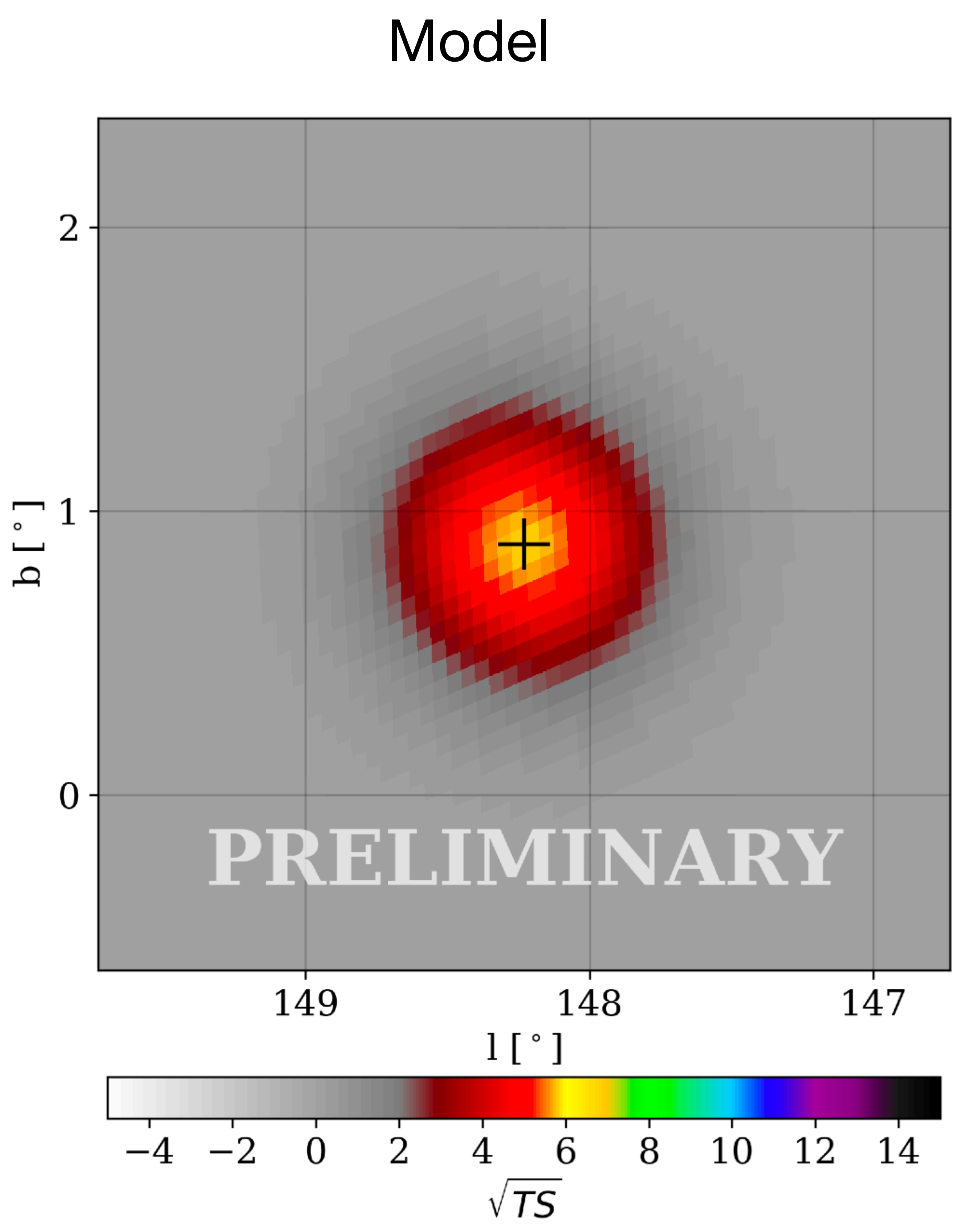

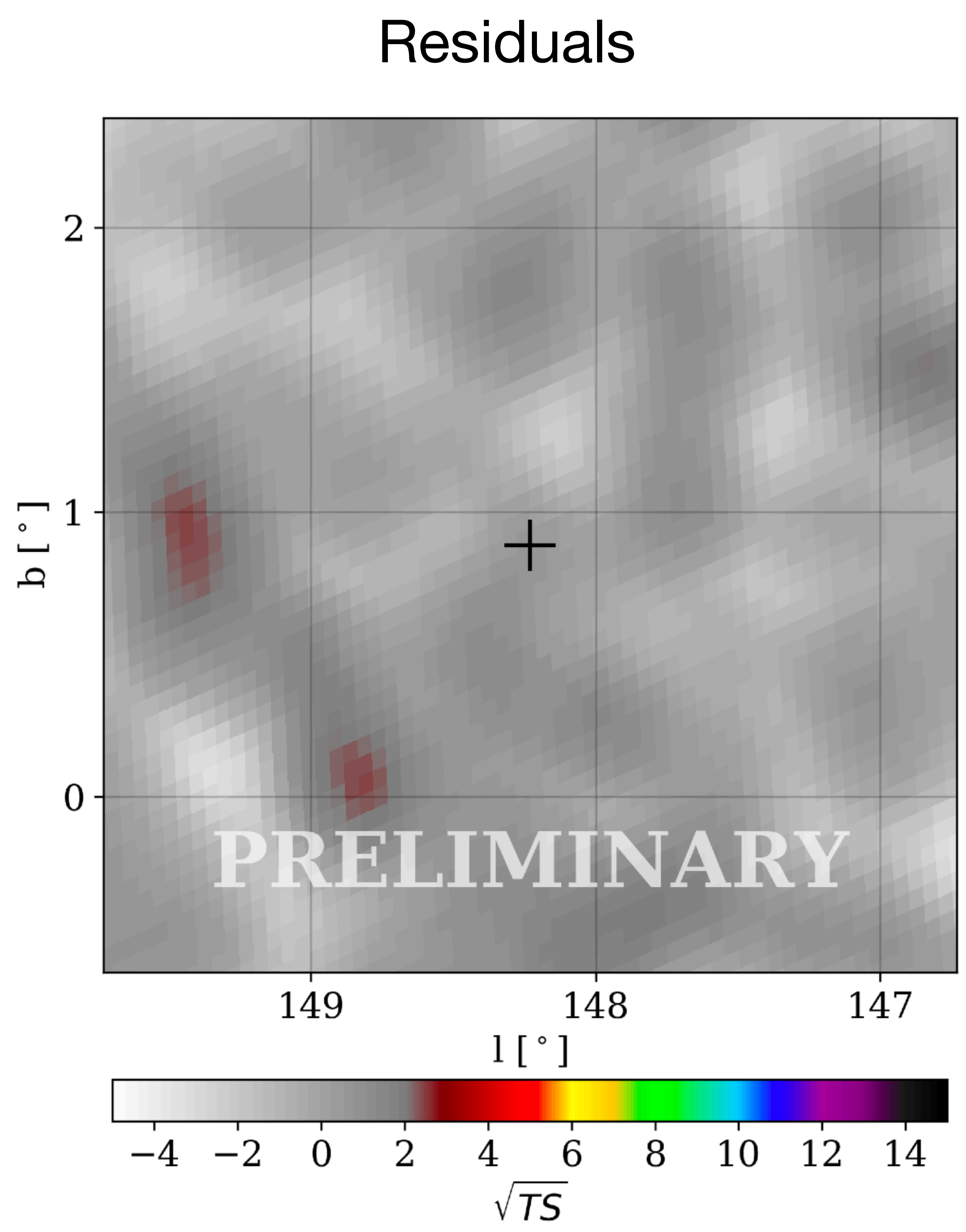

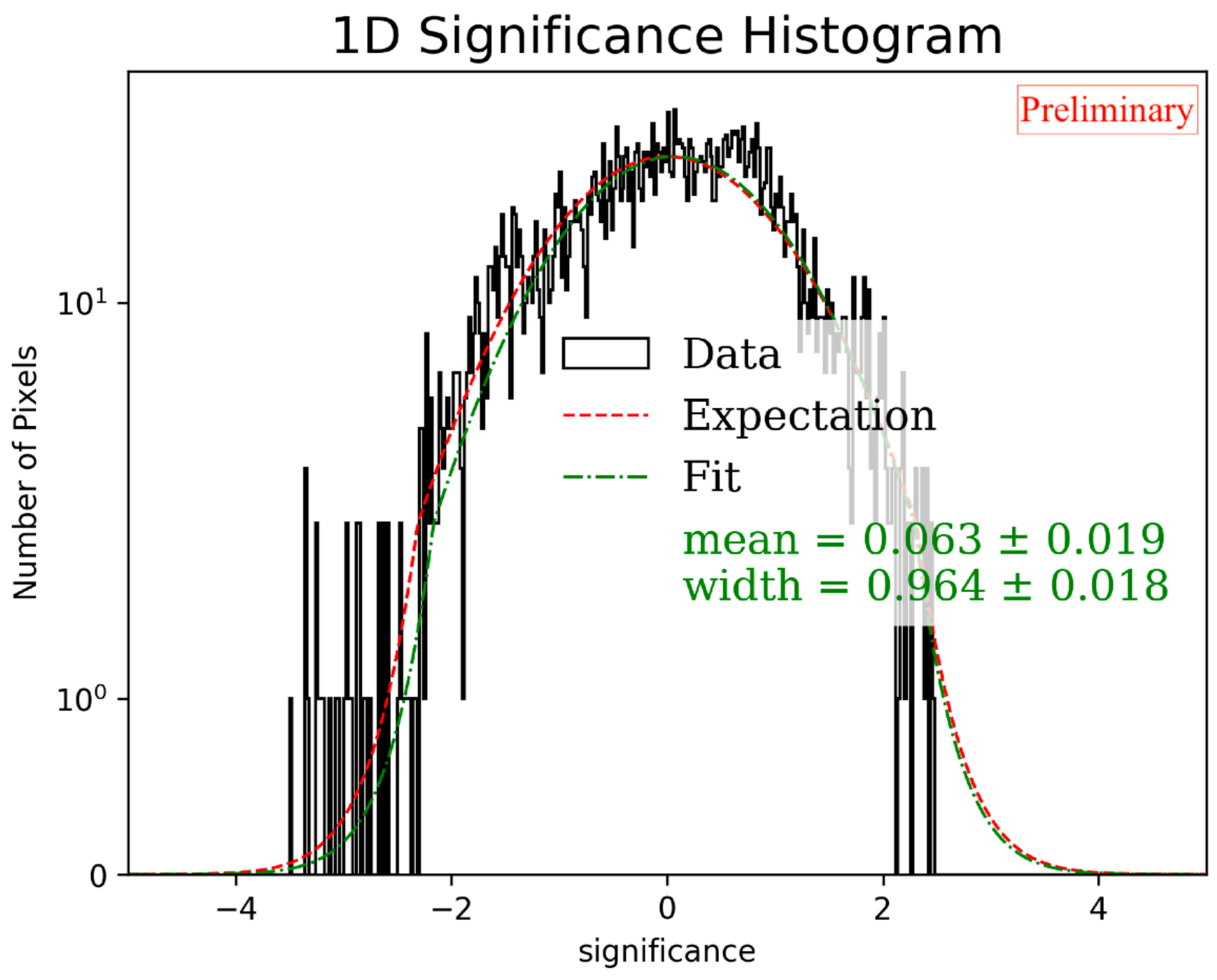

J0359 spectral energy distribution

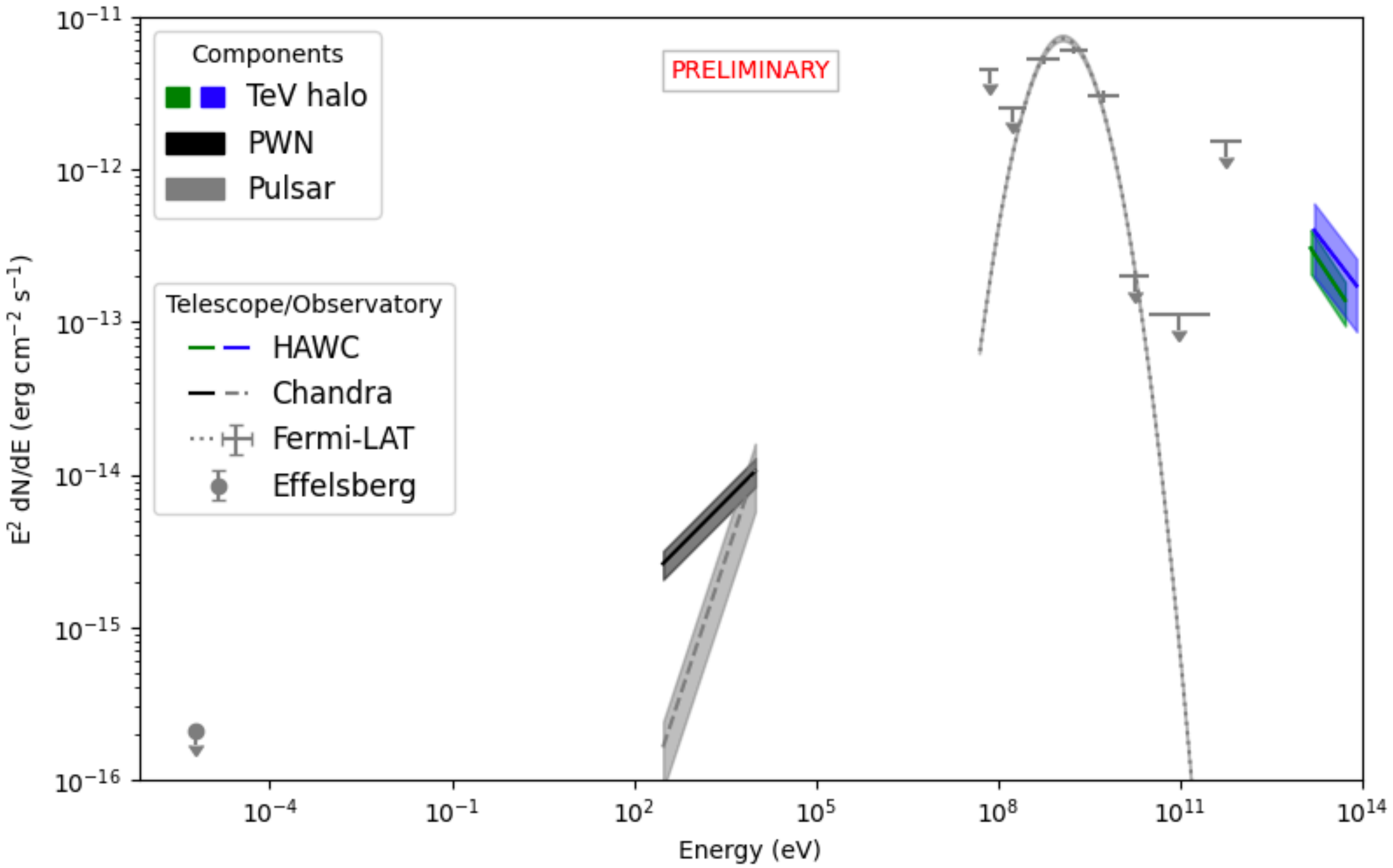

$$L_{VHE} = 1.8 \times 10^{31}\,\mathrm{erg\,s^{-1}} > L_X = 2 \times 10^{30}\,\mathrm{erg\,s^{-1}}$$

-> VHE emission might be from a different nature compared to the nebula, and is probably more extended than the X-ray PWN.

So, considering the luminosity and extension, the VHE excess is likely a TeV halo associated to PSR J0359+5414.

Upper limits on the diffusion coefficient

Taking 95% upper limits on J0359's extension (0.41°), the diffusion coefficient is $D = 3.7 \times 10^{27}$ cm$^2/s$, for an electron energy of ~100 TeV and electron cooling time of ~10 kys.

This value is very similar to one found for Geminga, $D = 4.5 \times 10^{27}$ cm$^2/s$ (Abeysekara et al. 2017).

PSR B0355+54

Radio-loud pulsar very close (5'.5) to J0359.

B0355 has not been detected at high and very-high energies (Benbow et al. 2021).

Due to the HAWC's angular resolution we can not discard a contribution from B0355.

However, the upper limits set by VERITAS are lower by ~2-3 times than the extrapolation of the HAWC's flux at 10 TeV. —> the excess emission is likely associated with J0359

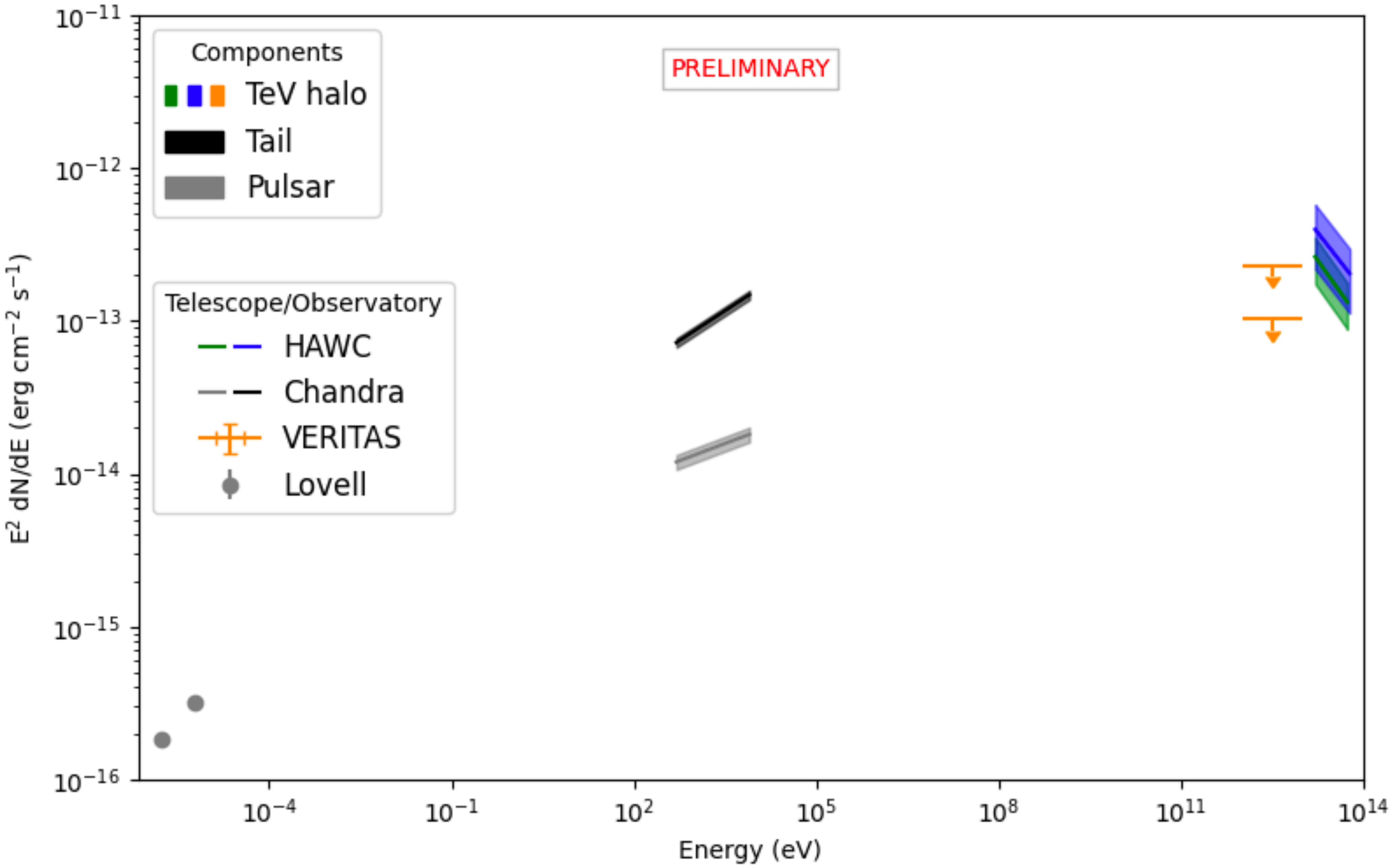

PSR B0355+54

B0355 scenario

Spatial model	TS	ΔBIC	Extension [°]	N_0 $\mathrm{TeV^{-1}\ cm^{-2}\ s^{-1}}$	α
Point-like	35.86	1.9	0.0	$(1.28^{+0.34}_{-0.27}) \times 10^{-16}$	2.56 ± 0.17
Extended	41.83	1.5	0.22 ± 0.09	$(2.0^{+0.7}_{-0.5}) \times 10^{-16}$	2.51 ± 0.15

ΔBIC is obtained comparing the BIC value with the best spectral model fit for both spatial models assuming that the emission is coming from J0359

J0359 + B0355 scenario

Two-source model	Source	TS	ΔBIC	Extension [°]	N_0 $\mathrm{TeV^{-1}\ cm^{-2}\ s^{-1}}$	α
	J0359	2.32		0.0	$(1.0^{+0.5}_{-0.9}) \times 10^{-16}$	$2.63^{+0.6}_{-0.20}$
Model A	B0355	0.32	24	0.0	$(0.00034^{+6}_{-0.00024}) \times 10^{-13}$	$2.4^{+1.3}_{-5}$
	J0359	8.73		$1.500^{+0.18}_{-0.004}$	$(3.3^{+1.5}_{-3.3}) \times 10^{-16}$	$2.2^{+0.4}_{-1.3}$
Model B	B0355	10.29	26	$0.14^{+0.08}_{-0.15}$	$(1.5^{+0.5}_{-0.4}) \times 10^{-16}$	2.56 ± 0.20
	J0359	13.02		1.5000 ± 0.0010	$(0.04^{+4}_{-0.04}) \times 10^{-14}$	2.2 ± 2.8
Model C	B0355	8.62	26 / 15	0.0	$(3.2^{+3.0}_{-1.5}) \times 10^{-16}$	2.60 ± 0.28

Model A —> two point-like sources
Model B —> two extended sources
Model C —> J0359 extended & B0355 point-like

ΔBIC is obtained comparing the BIC value with the best spectral model fit for both spatial models assuming that the emission is coming from J0359

Conclusions

- We detect a TeV halo candidate near the Galactic plane in a region that is not crowded that is likely associated to the radio-quiet pulsar PSR J0359+5414.

- This TeV halo candidate shares similar characteristics to others, suggesting that TeV halos could be a general feature of middle-age pulsars.

- It is important to perform multi-wavelength observations to confirm the finding.

Thank you

scoutino@icecube.wisc.edu

Picture credit: Avid González Muñoz

Backup

TeV halo candidate list from the Third HAWC Catalog (3HWC, Albert et al. 2020) for a 1523-day data set (November 2014, June 2019)

HAWC	l (°)	b (°)	Pulsar	Age (kyr)	$\dot{E}$ (erg s^{-1})	Distance (kpc)	Separation (°)	TeVCat
3HWC J0540+228	184.58	−4.13	B0540+23	253.0	4.09e+34	1.56	0.83	HAWC J0543+233
3HWC J0543+231	184.67	−3.52	B0540+23	253.0	4.09e+34	1.56	0.36	HAWC J0543+233
3HWC J0631+169	195.63	3.45	J0633+1746	342.0	3.25e+34	0.19	0.95	Geminga
3HWC J0634+180	195.00	4.62	J0633+1746	342.0	3.25e+34	0.19	0.38	Geminga Pulsar
3HWC J0659+147	200.60	8.40	B0656+14	111.0	3.8e+34	0.29	0.51	2HWC J0700+143
3HWC J0702+147	200.91	9.01	B0656+14	111.0	3.8e+34	0.29	0.77	2HWC J0700+143
3HWC J1739+099	33.89	20.34	J1740+1000	114.0	2.32e+35	1.23	0.13	...
3HWC J1831-095	22.13	0.02	J1831−0952	128.0	1.08e+36	3.68	0.27	HESS J1831-098
3HWC J1912+103	44.50	0.15	J1913+1011	169.0	2.87e+36	4.61	0.31	HESS J1912+101
3HWC J1923+169	51.58	0.89	J1925+1720	115.0	9.54e+35	5.06	0.67	...
3HWC J1928+178	52.93	0.20	J1925+1720	115.0	9.54e+35	5.06	0.85	2HWC J1928+177
3HWC J2031+415	80.21	1.14	J2032+4127	201.0	1.52e+35	1.33	0.11	TeV J2032+4130

Note. The age of the pulsar in kyr and the spin-down luminosity, $\dot{E}$, in erg s^{-1} are also given. The Separation column indicates the angular distance between the HAWC source and the ATNF pulsar (Manchester et al. 2005). The TeVCat column lists the previously detected TeV counterpart of each source.

Analysis method

Maximum likelihood analysis using the Multi-Mission Maximum Likelihood (3ML) framework (Vianello et al. 2015) with the HAWC Accelerated Likelihood (HAL) plugin.

In order to know which model best describes the observations, we use the likelihood ratio tests statistics (TS) as

$$TS = 2\ln\frac{\mathscr{L}_{\mathrm{S+B}}}{\mathscr{L}_{\mathrm{B}}}$$

$\mathscr{L}_{\mathrm{S+B}}$ —> maximum likelihood of the signal plus background model that depends on the spectral and spatial parameters assumed to describe the data.

$\mathscr{L}_{\mathrm{B}}$ —> maximum likelihood of the background-only hypothesis.

Analysis method

The Bayesian Information Criterion (BIC) is used to determine which model is preferred, which takes into account the number of free parameters in the fit.

When we compare two models, the difference in the BIC value, $\Delta\mathrm{BIC}$, quantifies the evidence against the model with a higher BIC value.

According to Kass & Raftery (1995), if $\Delta\mathrm{BIC}$ is between 0 and 2 it is not clear which model is preferred; however if $\Delta\mathrm{BIC}$ is between 2 and 6 the model with the smallest BIC value is preferred; even more, when $\Delta\mathrm{BIC} > 10$.

Diffusion model

Positrons and electrons diffuse away from the pulsar and is described by:

$$\frac{dN}{d\Omega} = \frac{1.22}{\pi^{3/2}\theta_{\rm d}(E)(\theta + 0.06\theta_{\rm d}(E))} \times \exp\left[-\frac{\theta^2}{\theta_{\rm d}(E)^2}\right],$$

where Ω denotes the solid angle, θ is angle from the source and $\theta_{\rm d}$ is the diffusion angle and is related to the diffusion radius $R_{\rm diff}$ by,

$$\theta_{\rm d} = \frac{180}{\pi}\frac{R_{\rm diff}}{d_{\rm src}},$$

where $d_{\rm src}$ is the distance to the source from Earth. This way the diffusion radius is defined as:

$$R_{\rm diff} = 2\sqrt{D(E_{\rm e})t_{\rm e}},$$

where D is the diffusion coefficient for electrons at energy $E_{\rm e}$ and $t_{\rm e}$ is electron cooling time (Abeysekara et al. 2017).